

PALSAR INTERFEROMETRY APPLIED TO THE ERUPTIONS OF EYJAFJALLAJÖKULL VOLCANO, ICELAND IN 2010

PI No 93

Kurt L. Feigl¹, Syed Tabrez Ali¹, Freysteinn Sigmundsson²

¹Department of Geoscience, University of Wisconsin-Madison, USA

²Nordic Volcanological Centre, Institute of Earth Sciences, University of Iceland

1. INTRODUCTION

The eruption of Eyjafjallajökull volcano in Iceland prompted many challenging questions, ranging from the fundamental — “How do volcanic eruptions begin?” — to the practical — “Will the ash cloud cancel my flight?” These questions lead to many others involving coupled dynamic processes. Can stresses from earthquakes, intrusive events, or other volcanoes trigger an eruption? When does exsolution by cooling increase the pressure of volatile gases sufficiently to propel magma upwards? Can hydrothermal fluids generate a triggering instability? Which processes control the height and duration of the ash plume, and thus its impact on air traffic, weather, and climate?

Eyjafjallajökull means “the glacier on the mountains next to the islands” [Einarsson, 2010]. Before erupting in March 2010, it had been exhibiting intermittent unrest for the previous 18 years [Sigmundsson et al., 2010]. In January 2010, the edifice began to inflate rapidly, as indicated by GPS and InSAR measurements [Sigmundsson et al., 2010]. On March 20th, the volcano erupted and the inflation essentially halted. This eruption on the rocky flank of the volcano continued through April 12th without ejecting material into flight paths. After a 2-day pause, the volcano erupted again on April 14th, from a vent on the summit, generating a plume over 6000 m in height [VAAC, 2010].

At Eyjafjallajökull, the mixing of two distinct types of magma appears to have triggered the ash-producing summit eruption in April 2010 [Sigmundsson et al., 2010]. As sketched in Figure 1, the flank eruption produced weakly alkalic olivine basalt (drawn in orange) that indicates a short residence time in the crust [Sigmundsson et al., 2010]. In contrast, the summit eruption produced trachyandesite (drawn in yellow), indicating a source that is distinct from those inferred for the intrusive episodes in 1994 and 1999 (drawn in red). Such bimodal volcanism also occurred during the 1996 eruption of Karymsky, when andesite erupted from the main vent and basalt from a flank [Eichelberger et al., 2006]. Other examples of magma-triggered eruptions [Sparks et al., 1977] include Askja 1875 [Sigurdsson and Sparks, 1981], Krafla 1975-84 [Tait et al., 1989], Pinatubo 1991 [Pallister et al., 1992]

and Santa Maria 1902 [Williams and Self, 1983]. One explanation for magmatic triggering involves a low-density layer “capturing” a magmatic intrusion and requiring pressure to build before the magma can ascend towards higher levels [Taisne and Jaupart, 2009]. Alternatively, the temperature contrast may exsolve volatile gases as the two types of magma mix together [Keiding and Sigmarsson, 2010; Moune et al., 2010; Sigmarsson et al., 2010].

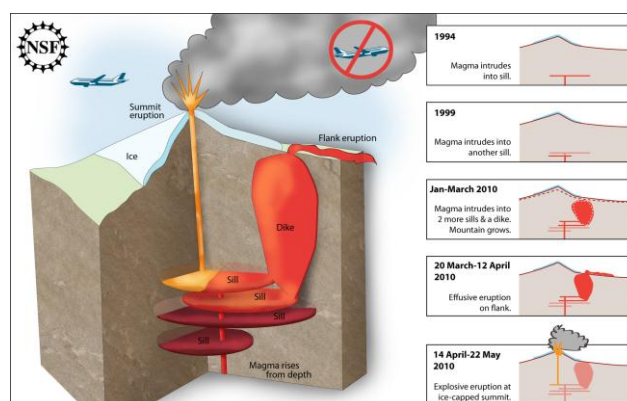


Figure 1. Artist's conception illustrating the three-dimensional geometry of the plumbing (left) and timing of events (right column) at Eyjafjallajökull volcano in Iceland. The interconnected sills and dikes are inferred from inversions of InSAR and GPS data [1-4]. The 1st, 2nd, and 3rd panels show distinct episodes of magmatic intrusions that caused measurable deformation and seismic events — but no eruptions — in 1994, 1999, and in the first 13 weeks of 2010. Each intrusive episode involved a different section of the plumbing, drawn in red and modelled as sills at depths of 5–7 km. The 4th panel illustrates the first eruption, between 20 March and 12 April 2010, when basaltic magma (orange) erupted onto the flank. The 5th panel shows the second eruption, between 14 April and 22 May, when a trachyandesitic magma (yellow), erupted explosively at the ice-capped summit (1600 m elevation). The ash plume rose to the 30,000-foot flight level and disrupted air traffic. Illustration by Zina Deretsky, NSF, commissioned by NSF to coincide with the publication of Sigmundsson et al. in *Nature* in November 2010.

2. DATA AND METHODS

We analyze synthetic aperture radar images acquired by the PALSAR sensor aboard the ALOS satellite. To generate the interferograms, we use the Diapason InSAR processing software [2006] developed by the French Space Agency, CNES. The topographic contribution to the interferograms was removed using a digital elevation model (DEM) that has been resampled to 100 m posting and 20 m accuracy [5]. The observed wrapped phase change values for the best pair spanning the eruptions in 2010 appears in Figure 2. In these interferograms, one fringe of phase change corresponds to 112 mm of range change in the direction of the satellite. The principle signal in the interferograms is a concentric fringe pattern consistent with volcanic deformation.

To build a data set for the inversion, we calculate the gradient of range change while simultaneously resampling (but not unwrapping) with a quadtree algorithm [Feigl and Sobol, manuscript in preparation, “PHA2QLS.C: a computer program to compress images of wrapped phase by simultaneously estimating gradients and quadtree resampling”]. Unlike wrapped phase change, the range gradient is continuous and differentiable, as pointed out by Sandwell and Price [6]. Using the gradient of range change as an observable quantity avoids all the pitfalls of phase unwrapping, as discussed by Feigl and Thurber [7]. While range change is one component of the displacement vector, its gradient is one component of the strain tensor. In absolute value, the largest range change gradient in the Eyjafjallajökull dataset is of the order of $\sim 20 \times 10^{-6}$, corresponding to a difference of 20 mm in range change over the 100 m distance between adjacent pixels in the interferogram. The fundamental condition for useful measurement of InSAR implies that the horizontal gradient of wrapped range change must not exceed half a fringe per pixel in absolute value [8]. For strains larger than this “gradient limit”, the corresponding pixel in the interferogram will show no correlation and will thus be excluded by the quadtree resampling.

To quantify the misfit between the observed and modeled values of the range gradient, the objective function calculates the cost as the absolute value of their difference, averaged over all samples. To minimize the objective function, we employ a simulated annealing algorithm, as part of the General Inversion of Phase Technique (GIPhT) [7]. We apply the strategy to estimate parameters of the plumbing system beneath Eyjafjallajökull volcano.

To describe the deformation, we consider an idealized half space with uniform elastic properties. We evaluate four different analytic descriptions of the source including:

- (a) a spherical volume, as originally formulated by Mogi [9] and later expressed by Segall [10] (Figure 3).
- (b) a rectangular sill with opening, as formulated by Okada [11] (Figure 4).
- (c) a horizontal circular disk, as formulated by Sun [12] (Figure 5).
- (d) a prolate spheroid, as formulated by Yang [13] (Figure 6).

3. RESULTS

Table 1 shows the quality of the fit of each of the four source models to the observed phase gradient values in terms of the mean deviation. Results suggest a source at a depth between 5 and 7 km.

Table 1. Comparison of models

| Name | Figure | Mean deviation (cycles/pixel) |
|------------------|----------|-------------------------------|
| Mogi sphere | Figure 3 | 0.0109 |
| Okada sill | Figure 4 | 0.0107 |
| Sun disk | Figure 5 | 0.0109 |
| Prolate spheroid | Figure 6 | 0.0107 |

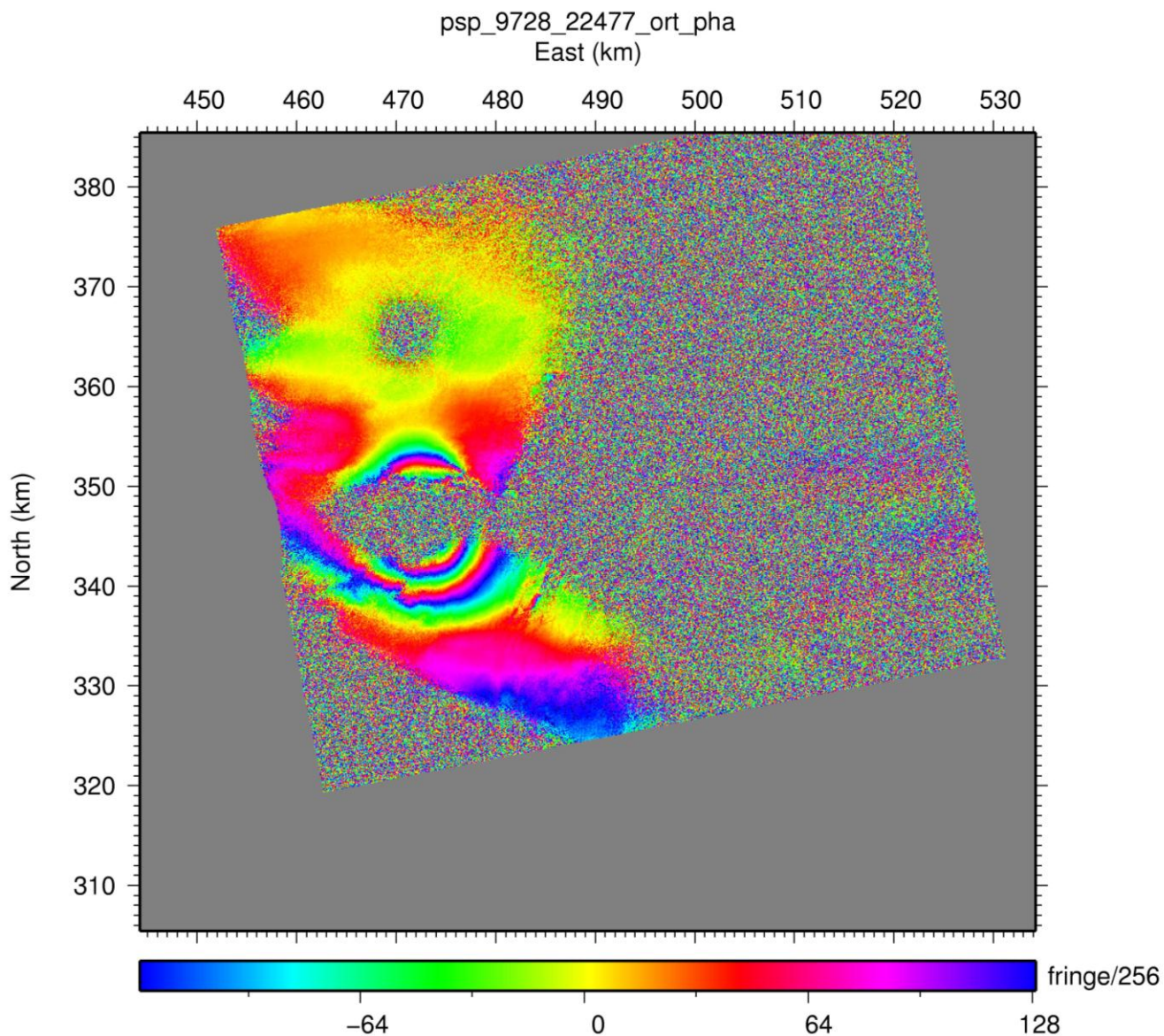


Figure 2. Interferogram for Eyjafjallajökull spanning the 874-day time interval from 2007-NOV-21 to 2010-APR-13 (ALOS orbit numbers 9728 and 22477). The images were acquired in path 16, frame 1270 in FBS mode. The altitude of ambiguity for the interferogram is 243 meters. One fringe corresponds to one cycle of phase change, or 118 mm of range change

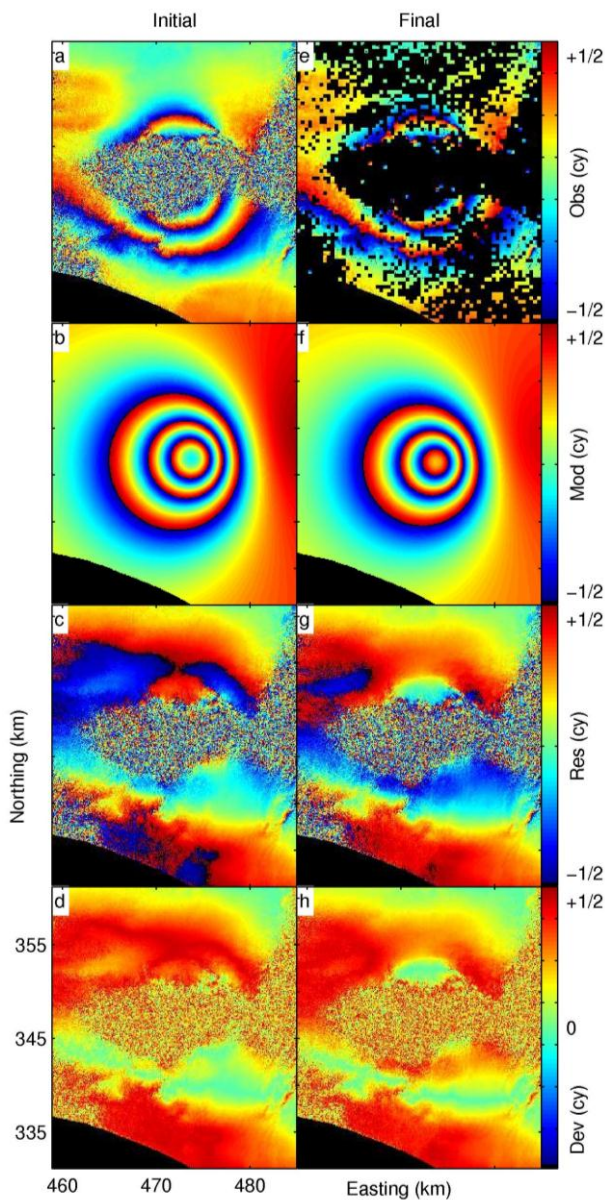


Figure 3. Interferograms for Eyjafjallajökull spanning the 874-day time interval from 2007-NOV-21 to 2010-APR-13. The panels include (a) observed phase; (b) modeled phase calculated from the initial estimate of the 4 free parameters in the Mogi model of a spherical source; (c) initial residual phase; (d) angular deviations for the initial estimate; (e) observed phase, as resampled by a quadtree algorithm; (f) modeled phase calculated from the final estimate; (g) final residual phase; and (h) angular deviations for the final estimate. In the upper three rows, one fringe corresponds to one cycle of phase change, or 118 mm of range change. In the bottom row, the colors denote the angular deviation in phase between 0 and 1/2 cycle. Coordinates are UTM easting and northing in km. Black areas indicate zero deformation and/or missing data (e.g, over the Atlantic Ocean to the south).

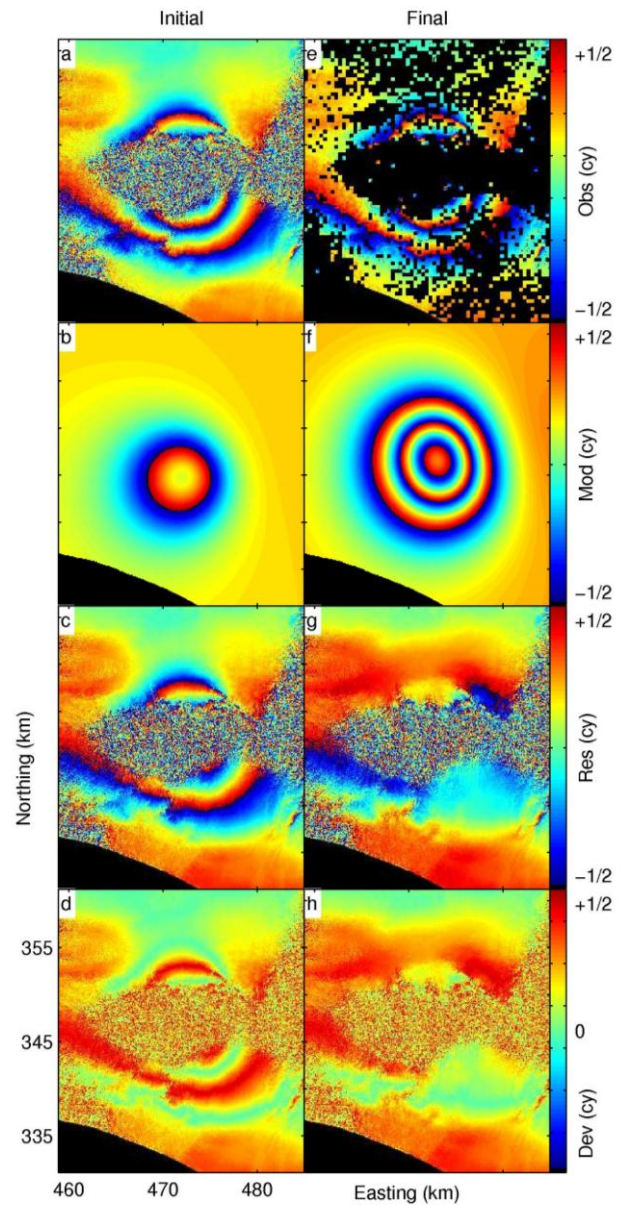


Figure 4. Interferograms using the Okada formulation for a rectangular sill. Plotting conventions as in previous figure.

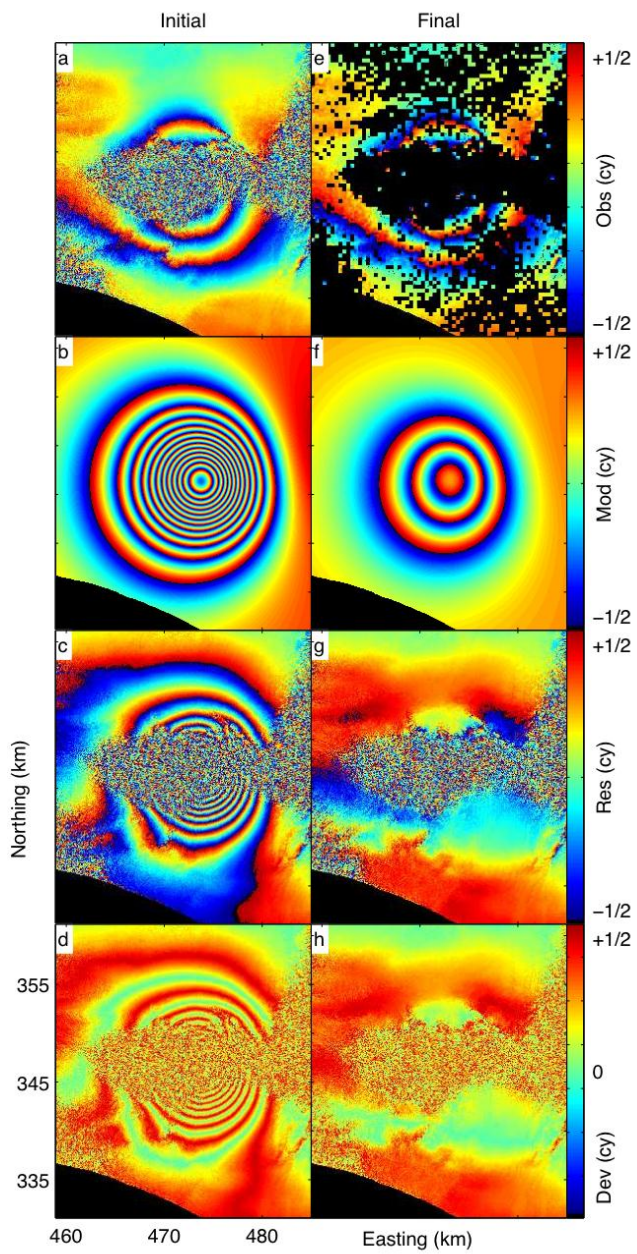


Figure 5. Interferograms using the Sun formulation for a horizontal disk-shaped sill. Plotting conventions as in previous figure.

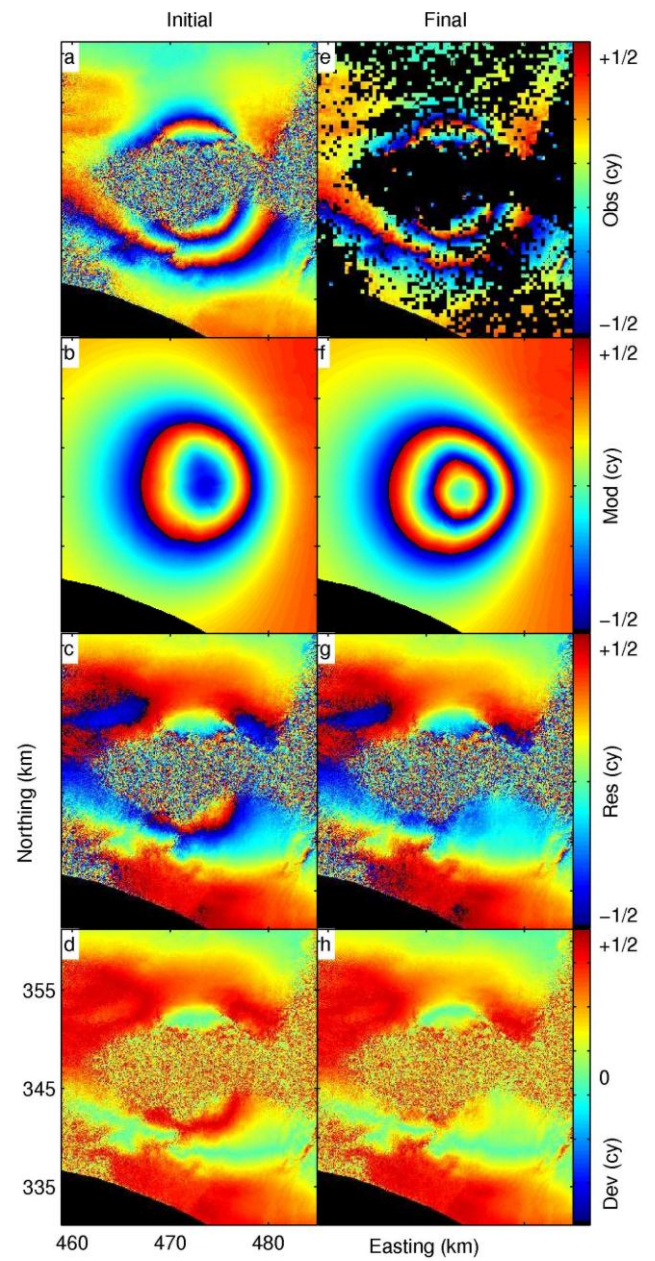


Figure 6. Interferograms using the Yang formulation for a prolate spheroid. Plotting conventions as in previous figure.

4. REFERENCES

- [1] R. Pedersen and F. Sigmundsson, "InSAR based sill model links spatially offset areas of deformation and seismicity for the 1994 unrest episode at Eyjafjallajökull volcano, Iceland," *Geophys. Res. Lett.*, vol. 31, p. 14610, July 1, 2004.
- [2] F. Sigmundsson, S. Hreinsdóttir, A. Hooper, T. Arnadóttir, R. Pedersen, M. J. Roberts, N. Oskarsson, A. Auriac, J. Decriem, P. Einarsson, H. Geirsson, M. Hensch, B. G. Ófeigsson, E. Sturkell, H. Sveinbjörnsson, and K. L. Feigl, "Intrusion triggering of the 2010 Eyjafjallajökull explosive eruption," *Nature*, vol. 468, pp. 426-430, 2010.
- [3] R. Pedersen and F. Sigmundsson, "Temporal development of the 1999 intrusive episode in the Eyjafjallajökull volcano, Iceland, derived from InSAR images," *Bulletin of Volcanology*, vol. 68, pp. 377-393, 2006.
- [4] R. Pedersen, F. Sigmundsson, and P. I. Einarsson, "Controlling factors on earthquake swarms associated with magmatic intrusions; Constraints from Iceland," *Journal of Volcanology and Geothermal Research*, vol. 162, pp. 73-80, 2007.
- [5] K. Arnasson, "A Digital Elevation Model for Iceland with 25-m grid posting and 10-m accuracy," L. I. I. L. Survey), Ed., ed, 2006.
- [6] D. T. Sandwell and E. J. Price, "Multiple pass INSAR processing for geophysical applications: stack phase gradient then unwrap," in *Eos Trans. Amer. Geophys. Un. Meeting Suppl.* vol. 77, ed, 1996, p. F52.
- [7] K. L. Feigl and C. H. Thurber, "A method for modelling radar interferograms without phase unwrapping: application to the M 5 Fawnskin, California earthquake of 1992 December 4," *Geophysical Journal International*, vol. 176, pp. 491-504, 2009.
- [8] D. Massonnet and K. L. Feigl, "Radar interferometry and its application to changes in the Earth's surface," *Rev. Geophys.*, vol. 36, pp. 441-500, 1998.
- [9] K. Mogi, "Relations between the eruption of various volcanoes and the deformations of the ground surfaces around them," *Bull. Earthquake Research Institute*, vol. 36, pp. 99-134, 1958.
- [10] P. Segall, *Earthquake and volcano deformation*. Princeton, N.J.: Princeton University Press, 2010.
- [11] Y. Okada, "Surface deformation due to shear and tensile faults in a half-space," *Bull. Seism. Soc. Am.*, vol. 75, pp. 1135-1154, 1985.
- [12] R. J. Sun, "Theoretical size of hydraulically induced horizontal fractures and corresponding surface uplift in an idealized medium," *J. Geophys. Res.*, vol. 74, pp. 5995-6011, 1969.
- [13] X.-M. Yang, P. M. Davis, and J. H. Dieterich, "Deformation From Inflation of a Dipping Finite Prolate Spheroid in an Elastic Half-Space as a Model for Volcanic Stressing," *J. Geophys. Res.*, vol. 93, pp. 4249-4257, 1988.

5. ACKNOWLEDGEMENTS

"This material is based upon work supported by the U.S. National Science Foundation under Grant Nos. 0739014 & 1042103. Any opinions, findings, and conclusions or recommendations expressed in this material are those of the author(s) and do not necessarily reflect the views of the National Science Foundation."